Available online at www.sciencedirect.com
SCIENCE DIRECT
Journal of Crystal Growth 259 (2003) 343–351
JOURNAL OF CRYSTAL GROWTH
www.elsevier.com/locate/jcrysgro

Development of indium tin oxide film texture during DC magnetron sputtering deposition

Yeon Sik Jung*, Sung Soo Lee

R&D Center, Samsung Corning, 644, Jinpyoung-dong, Gumi, Kyoung-buk 730-725, South Korea

Received 11 July 2003; accepted 31 July 2003
Communicated by M. Schieber

Abstract

The indium tin oxide (ITO) film texture development process during sputtering deposition was explored. Cross-section TEM images revealed that prepared ITO films have columnar structures. $\theta - 2\theta$ X-ray diffraction (XRD) studies on ITO thin films deposited under various sputtering conditions were conducted. The change of XRD profiles with increasing thickness was monitored to elucidate the mechanism of film texture development. ITO films, which were deposited under conventional conditions, evolved to (4 0 0) orientation with increasing film thickness. In contrast, surplus amounts of additional oxygen gas flow suppressed growth of (4 0 0)-oriented grains. Meanwhile, moderate ranges of pressure and power density and higher substrate temperatures resulted in more (4 0 0)-oriented film textures. The development of texture to (4 0 0) orientation is attributed to a lower surface energy and a height advantage combined with shadowing effect. The ITO film growth process was assumed to be composed of two steps, the nucleation step and the evolution step. Higher adatom mobility is thought to be very important for the nucleation of (4 0 0)-oriented grains.

PACS: 68.55.Jk

Keywords: A1. Growth models; A1. X-ray diffraction; A3. Physical vapor deposition processes; B1. Oxides; B2. Semiconducting indium compounds

1. Introduction

Many kinds of transparent conducting oxide (TCO) films such as impurity-doped indium oxides, tin oxides, and zinc oxide systems have been widely used as transparent conductors for numerous opto-electronic applications [1–3]. Especially tin-doped indium oxide (ITO) thin films have been widely used due to low resistivity, high transmittance, and good etching properties [4,5].

Many researchers have reported a change of the preferred orientation of ITO thin films with varied process conditions [6–11], however, its development mechanism has not yet been fully discussed.

*Corresponding author. Koreas Institute of Science and Technology, Thin Films Research Center, 39-1 Hawolgok-dong, Seongbuk-gu, Seoul 136791 South Korea. Tel.: +82-54-470-7494, fax.: +82-54-470-7814.

E-mail address: ysjung@bomun.kaist.ac.kr (Y.S. Jung).

0022-0248/$ - see front matter © 2003 Elsevier B.V. All rights reserved.
doi:10.1016/j.jcrysgro.2003.07.006

Therefore, it is worthwhile to elucidate the mechanism of texture development since critical properties such as transmittance, surface roughness, etching rate, etc. have been found to be related with preferential orientation [11,12].

From a thermodynamic viewpoint, the preferred orientations of thin films are known to be the planes of lowest surface energy [13]. Also, from the viewpoint of kinetics, only grains with the highest growth-rate plane eventually survive [14,15].

Meanwhile, there have been many papers regarding development of the preferred orientation of thin films such as titanium nitride and chromium nitride [15–17]. To refer to them is one way to get a clue to the development of ITO film texture. In presentations from Pelleg et al. the preferred orientation of TiN thin films was controlled by competition between surface energy and strain energy [16]. A more recent result, however, showed that in-plane stresses are not necessary to explain the (1 1 1) preferred orientation of TiN thin films [17,18]. Li et al. suggested the preferred orientation of TiN films is developed by competition of grains with different orientations [15]. On the other hand, shadowing effect leads to higher growth rate of the grains with a height advantage [19].

Though there have not been sufficient discussions about the texture development of ITO thin films, many researchers presented the change of preferential orientation of ITO thin films with different deposition conditions. Some researchers reported that the orientation of the film changed from (4 0 0) to (2 2 2) as oxygen partial pressure increased during sputtering deposition [20]. It was reported that grain texture changed from (2 2 2) to (4 0 0) as the substrate temperature increased [10]. Kim et al. did not explicitly mention the enhanced peak intensity of (4 0 0) plane in their research, but their X-ray diffraction (XRD) patterns clearly showed that (4 0 0)/(2 2 2) peak intensity ratio increases with film thickness [8]. Though there have been controversial reports about the effect of sputtering pressure, (4 0 0) peak intensity mainly decreased as sputtering pressure increased [6,7].

In this study, we explore the development mechanism of ITO film texture. To do so, we performed a series of experiments varying DC magnetron sputtering parameters e.g. sputtering pressure, oxygen flow rate, sputtering power density, substrate temperature, and film thickness. We mainly discussed the influence of adatom mobility on film texture.

2. Experiments

ITO thin films were sputter-deposited using an ITO target in an in-line magnetron sputter-deposition system equipped with DC power suppliers. The chamber, which was equipped with a load-lock system and diffusion pumps, had a base pressure of 5×10^{-6} Torr. The target (128 mm $\times$ 450 mm) used was a sintered ITO containing 10 wt% SnO_2 (99.99%). Sputtering was carried out at a pressure of 0.1–3 Pa in pure Ar or Ar/O_2 gas mixture with varying sputtering parameters such as sputtering pressure, power density, oxygen flow rate and deposition temperature. The deposition temperature was usually 200°C except the sample to investigate the effect of temperature. The films were deposited on soda-lime glass substrates, which were placed 50 mm apart and parallel from the target surface. The substrates were cleaned in an ultrasonic bath in 4% Deconex 12PA at 65°C for 6 min, and then rinsed in deionized water in the ultrasonic bath for another 15 min. The target was pre-sputtered for 3 min. The thickness of the films ranged from 60 nm to 1 μm.

Conventional $\theta - 2\theta$ X-ray diffraction studies on the films were carried out in a Philips PW1710 diffractometer using Cu Kα radiation ($\lambda = 1.5405$Å). Film density was measured by X-ray reflectometry (D8DISCOVER, Bruker) technique. Samples for cross-section TEM observation were prepared by cutting and mechanical grinding to 100 μm before dimpling (Model 656, Gatan). Additionally, low angle ion milling was carried out using an ion miller (Lamp 1010, Fischione). A JEM 4010 JEOL microscope with a point resolution of 0.15 nm was used to perform the TEM analysis.

3. Results and discussions

3.1. Texture development of ITO films with increasing thickness

Figs. 1a–c shows the observed cross-sectional TEM images of ITO thin films deposited at 200°C. Fig. 1 presents the zone 2 (columnar) structure proposed by Thornton [21]. As shown in Fig. 1b, the atomic layers were grown continuously from the bottom of each grain, which means the orientation of each grain was maintained during film growth. Thin films of a columnar structure usually have a preferred orientation because of the different growth rate of each grain [22]. Columnar structures have been found to be observed when the mobility of deposited atoms is limited [23]. Meanwhile, each grain maintained the crystallographic orientation of the initial growth stage, which means secondary nucleation seldom took place during columnar growth.

Fig. 2a shows XRD patterns for ITO films as a function of film thickness. The relative portion of (2 2 2) peak intensity ($I_{(222)}/(I_{(222)}+I_{(400)})$) depending upon film thickness was shown in Fig. 2b. Though the value was never exactly same as the true portion of (2 2 2) grains, it could be an indirect measure of the portion. The films were deposited at 0.15 Pa with no additional flow of oxygen gas, and these conditions would be close to the general conditions for ITO films deposition since oxygen gas below several percents of Ar gas flow is usually used to achieve good electrical and optical properties. The relative (4 0 0) peak intensity increased significantly as film thickness increased. The two figures clearly show that the ITO films evolved to (4 0 0) orientation with increasing film thickness. Similar results can be found in other research [8].

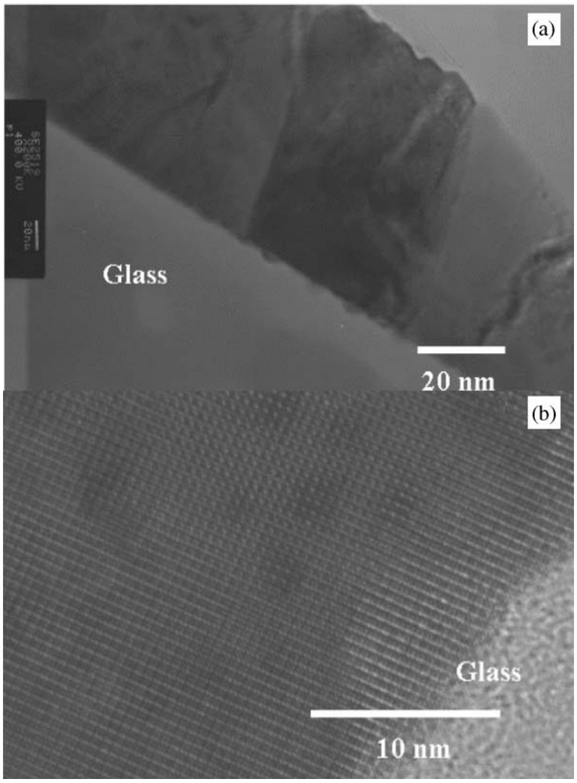

Fig. 1. Cross-sectional TEM images of ITO films deposited on glass substrates.

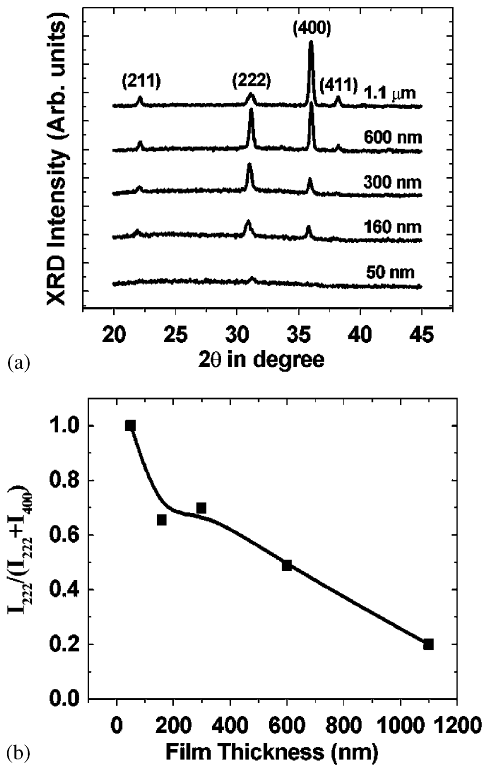

Fig. 2. Change of: (a) XRD profiles and (b) ($I_{(222)}/(I_{(222)}+I_{(400)})$) depending upon film thickness (no oxygen condition).

From the viewpoint of thermodynamics, the preferred orientations of thin films has been known to be the planes of the lowest surface energy [13]. In addition to that, shadowing effect and height difference of grains can be responsible for texture development [19]. Kamei et al. reported (4 0 0)-oriented grain in ITO thin films have higher thickness than other grains [24].

Figs. 3a and b exhibits the change of XRD profiles of ITO films deposited at 0.15 Pa with oxygen flow rate of 6 sccm and the relative portion of (2 2 2) peak intensity ($I_{(222)}/(I_{(222)}+I_{(211)})$) depending upon film thickness. The XRD profiles development feature was totally different from the case in Fig. 2. The (4 0 0) peak was not found for any of the samples, instead, the portion of (2 1 1) peak increased significantly at higher film thickness. In the case of surplus oxygen flow during deposition, only the nuclei with (2 2 2) and (2 1 1) orientations were formed at initial growth stage. By comparing with the XRD results shown in Fig. 2, where (4 0 0)-oriented grains are also identified, it can be concluded that oxygen flow rate considerably influences the nucleation step.

Additional experiments were performed to investigate how the initial deposition conditions affect the texture of the ITO films. During the deposition of samples whose XRD profiles are shown in Fig. 4a, no oxygen was supplied until 100 nm. Then, deposition was temporarily stopped, and pre-sputtering started with 6 sccm of oxygen gas flow into the chamber. After 3 min the film deposition process was restarted from the thickness of 100 nm with the same amount of oxygen gas. The XRD profiles of those samples

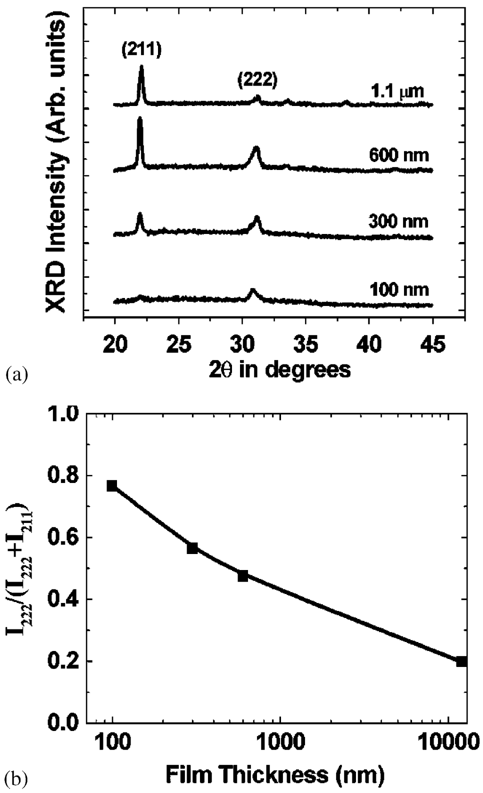

Fig. 3. Change of: (a) XRD profiles and (b) ($I_{(222)}/(I_{(222)}+I_{(400)})$) depending upon film thickness (oxygen flow of 6 sccm).

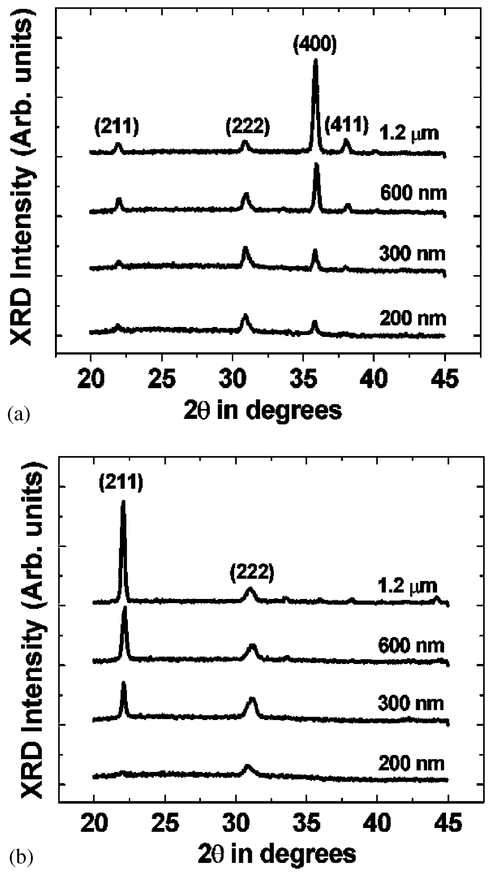

Fig. 4. Change of XRD profiles of the samples prepared with mixed conditions: (a) initially no oxygen, later 6 sccm and (b) initially oxygen flow of 6 sccm, later no oxygen.

were very similar to the results presented in Fig. 2a, where no oxygen was supplied during the entire film deposition process. For the samples of which XRD profiles are shown in Fig. 4b, the films were deposited in the opposite way. Until 100 nm, the films were deposited with oxygen gas of 6 sccm, and then oxygen flow was stopped. The deposition was restarted after pre-sputtering for 3 min. The XRD profiles of the samples were analogous to the result of Fig. 3a, where oxygen gas of 6 sccm was supplied during the entire film deposition process.

These results reveal the film texture development process is highly dependent on initial deposition conditions. Though deposition conditions were significantly changed after depositing 100 nm, development of film texture was similar as if deposition conditions were not changed for upper layers. Samples deposited with no oxygen flow initially had (4 0 0), (2 2 2), and (2 1 1) orientations, but samples with oxygen flow rates of 6 sccm had only (2 2 2) and (2 1 1) orientations, regardless of the conditions for upper layers. That shows the initially formed nuclei maintained their crystallographic orientation during growth, and secondary nucleation hardly takes place under the deposition conditions of this study. Deposition was performed at sputtering power density of 5.33 W/cm^2, under the sputtering pressure of 0.15 Pa, and at a deposition temperature of 200°C. These conditions are very typical in depositing ITO films.

Pelleg et al. proposed the (2 0 0) plane of TiN films has the lowest surface energy since the plane has the fewest number of broken bonds per unit area [16]. In the same way, (1 1 1) TiN film planes have the highest surface energy due to the fact that they are the most densely packed planes, which means a higher number of broken bonds. In the case of ITO films of bixbite, the (2 2 2) plane is known to be the most densely packed plane [25], as a result, it is the highest energy plane, whereas the (4 0 0) plane has the lowest energy. Of course, the lowest energy plane ((4 0 0)-orientation) will occupy more surface area with increasing thickness. In addition, height advantage of (4 0 0)-oriented grains can be a help to the higher growth rate of the grains.

3.2. Effects of sputtering conditions on XRD profiles

Fig. 5 shows the XRD profile of samples deposited with various oxygen gas flow rates. Deposition was performed at a sputtering power density of 5.33 W/cm^2, under the sputtering pressure of 0.15 Pa, and at a deposition temperature of 200°C. The sample thickness was about 150 nm, which is a typical thickness of ITO thin films for opto-electronic applications due to high transmittance. As the oxygen flow rate increased, the (2 2 2) preferential orientation became dominant. No (4 0 0) peak was observed above the oxygen gas flow rate of 2 sccm. The influence of sputtering pressure on XRD profiles is exhibited in Fig. 6. Fig. 6b shows the relative peak intensity of the (2 2 2) plane ($I_{(222)}/(I_{(222)}+I_{(400)})$) decreases until 0.7 Pa, and then increases steadily. (2 2 2)

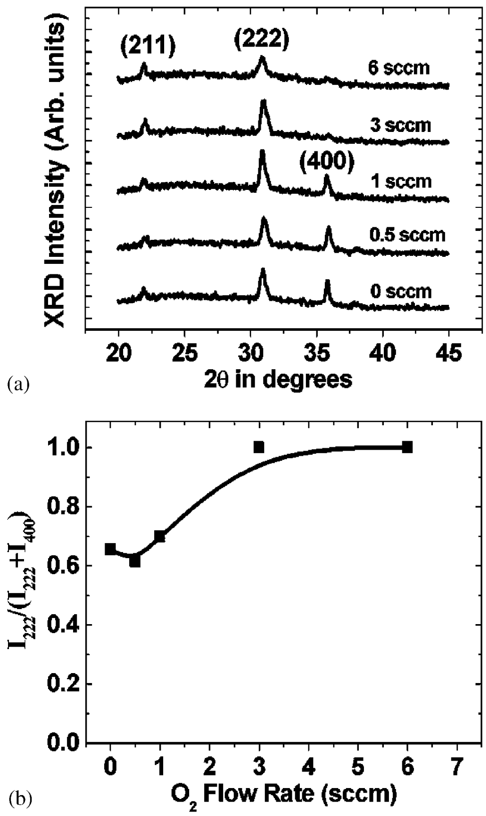

Fig. 5. Change of: (a) XRD profiles and (b) ($I_{(222)}/(I_{(222)}+I_{(400)})$) depending upon oxygen flow rate.

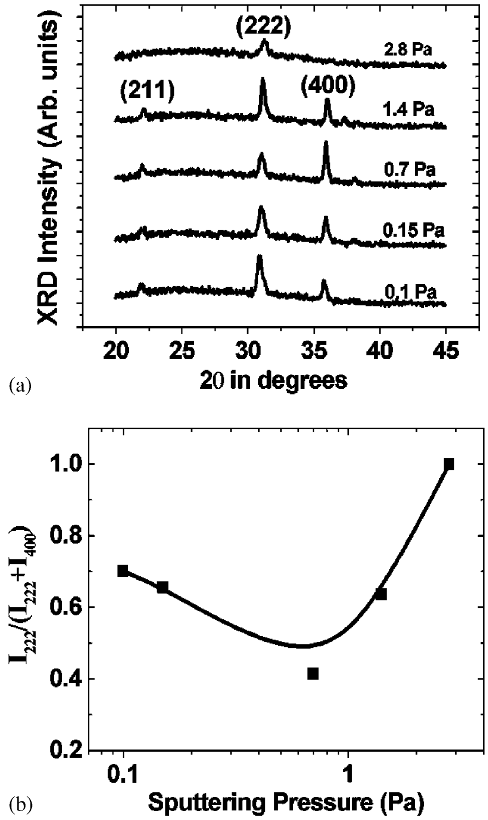

Fig. 6. Change of: (a) XRD profiles and (b) ($I_{(222)}$/($I_{(222)}+I_{(400)}$)) depending upon sputtering pressure.

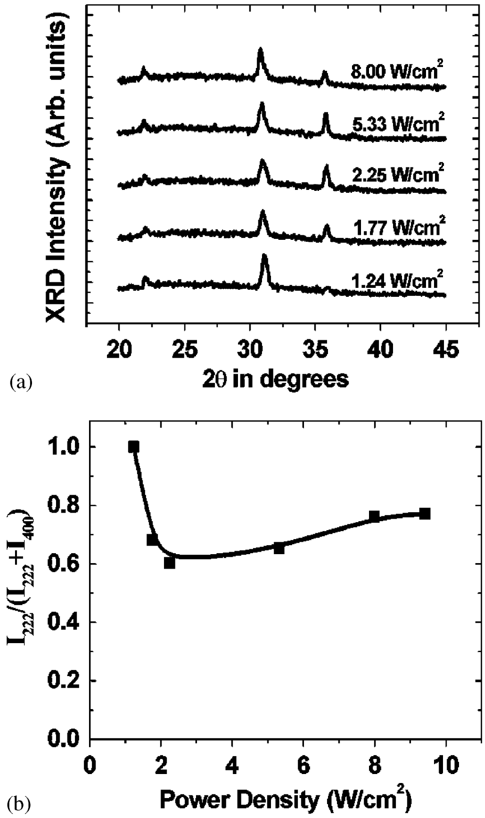

Fig. 7. Change of: (a) XRD profiles and (b) ($I_{(222)}$/($I_{(222)}+I_{(400)}$)) depending upon sputtering power.

peak was observed only at a very high sputtering pressure. Deposition was performed at a sputtering power density of 5.33 W/cm^2, without additional oxygen gas flow, and at a deposition temperature of 200°C. Fig. 7 shows the change of XRD profiles with increasing sputtering power. Deposition was performed at a temperature of 200°C, without additional oxygen gas flow. Films deposited at a very low sputtering power density had (2 2 2) preferred orientation, and the relative peak intensity of the (2 2 2) plane ($I_{(222)}$/($I_{(222)}+I_{(400)}$)) was lowest at a sputtering power density of 2.25 W/cm^2, and then increased slowly with increasing power density. Fig. 8 shows the XRD profile of samples deposited at various sputtering temperatures. Deposition was performed at a sputtering power density of 5.33 W/cm^2, under 0.15 Pa, without additional oxygen gas flow. As the substrate temperature increased, the peak intensities also increased, and the relative peak intensity of (4 0 0) planes noticeably increased.

Considerable parts of these phenomena have also been reported by other researchers. For instance, (2 2 2) peak became dominant with an increasing oxygen flow rate [20] and a decreasing substrate temperature [10], and those results are consistent with our data. Although not exactly the same, a very similar influence of sputtering pressure on the XRD profile was also reported [7]. However, the dominant factors and mechanisms for these texture development phenomena have not yet been fully understood. As mentioned previously in this study, the film texture of ITO depends on initial process conditions, and (4 0 0) orientation is thought to be thermodynamically favorable.

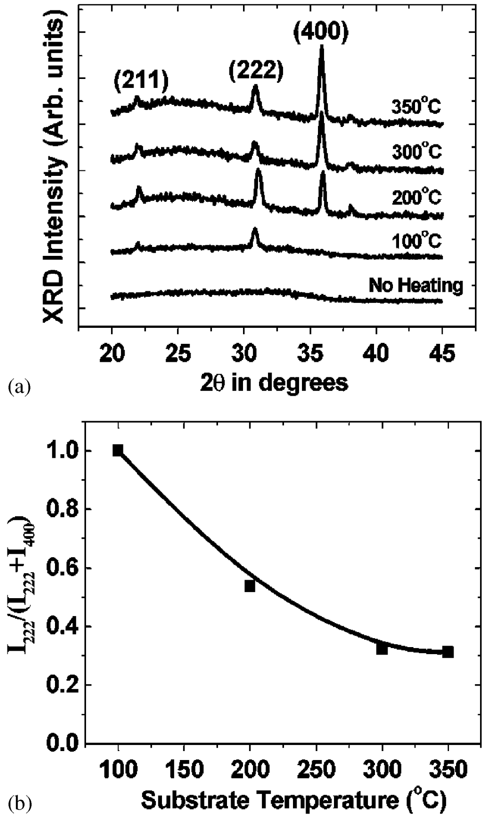

Fig. 8. Change of: (a) XRD profiles and (b) ($I_{(222)}$/($I_{(222)}+I_{(400)}$)) depending upon substrate temperature.

On the other hand, the actual crystallographic orientations of ITO thin film are very different depending upon deposition conditions. Actually in many cases, ITO films have (2 2 2) preferred orientation, which is not expected to be thermodynamically favorable. We can distinguish the usual film growth process into two steps. The first step is the nucleation process, and the second is the film development process. The film texture at a certain thickness is thought to be dependent on the initial orientations of grains and the speed of texture development into a preferred orientation.

The degree of orientation of the (4 0 0) plane is expected to be dependent on the mobility of adatoms on the substrate or the film. The diffusivity of adatoms on the surface of films can be expressed in the following equation, and the adatom mobility would be proportional to this value [26]

$$D_s = (1/2)a_0^2 v \exp(-E_s/kT), \tag{1}$$

where a_0 is atomic dimension, v the vibrational frequency of adatoms and E_s the activation energy for surface diffusion. The mean square distance traveled by a diffusing adatom in a time t would be expressed as follows [26]:

$$\langle X^2 \rangle = 2D_s t. \tag{2}$$

If adatoms on substrate have a sufficient amount of energy, then they would form nuclei that have thermodynamically favorable (4 0 0) orientations. Even though a (2 2 2)-oriented nucleus is shorter in distance, if an adatom has higher energy, then it would have a higher possibility of being attached to a (4 0 0)-oriented nucleus than the case of lower energy. Consequently, ITO films would have a higher portion of (4 0 0)-oriented nuclei under process conditions for higher adatom mobility. The average energy of adatoms is thought to be determined by the kinetic energy of sputtered atoms just before arriving on substrates, Ar^+ ion bombardment energy and substrate temperature. Ar^+ ions that are incident on the substrate or film surface can supply a considerable amount of energy to the adatoms that have not yet settled [27].

Meanwhile, regardless of oxygen flow rates, (2 2 2) the orientation of grains is very dominant in ITO films of small thickness, as shown in Figs. 2 and 3. The features of texture development with increasing thickness were quite different depending on the oxygen flow rate. However, (2 2 2) preferential orientation is highly dominant at the initial growth stage for any deposition conditions. These results may stem from the crystal structure of indium metal. Indium has a face-centered tetragonal structure, in which the (1 1 1) plane is the most densely packed plane, and consequently the lowest energy plane. Metallic thin films of FCC structure such as Ag, Cu and Al show (1 1 1) preferred orientation [28], which is perpendicular to the most densely packed plane. At the nucleation stage of ITO thin films, indium atoms on substrate are likely to aggregate into densely packed (1 1 1) planes, which are very close to (2 2 2) planes in bixbite structure. Banerjee et al. introduced a similar explanation for TiN thin film growth [17]. They attributed the (1 1 1) orientation in TiN films to the consequence of kinetically limited growth, where Ti atoms are thought to be aggregate into low energy forming {1 1 1} planes. That mechanism can be applied quite well to the (2 2 2) preferred orientation in ITO films.

With increased oxygen partial pressure during sputtering, more oxygen atoms would be absorbed on the substrate or film surface. As a result, the metal adatoms are likely to be easily trapped by the oxygen atom, and average adatom mobility and diffusion length will decrease under high oxygen partial pressure. Thus, the nucleation step is more kinetically limited, and (2 2 2) orientation becomes dominant.

In the moderate range of sputtering pressure (0.7 Pa), the degree of (4 0 0) orientation was highest, as shown in Fig. 6. This may have resulted from the competition of opposite two effects with varied sputtering pressure. At low pressure, the cathode sheath becomes broader, and thus increases the possibility that generated ions will collide on the chamber wall. As a result, the ions are easily neutralized, and ion density is relatively low. Meanwhile, a longer mean free path at low pressure results in higher kinetic energy of Ar^+ ions and sputtered atoms due to fewer scattering events. Chiu et al. proposed the product of ion flux and incident energy represents the resultant energy supplied by ion bombardment per deposited atoms [27]. At very low pressure, adatom mobility will be diminished in spite of higher ion energy because of low ion density. On the contrary, at very high pressure, lower ion energy due to frequent collision among neutral gases and ions results in very low adatom mobility. Consequently, low adatom mobility under very low and high sputtering pressure leads to more kinetically limited (2 2 2) orientation. However, in the moderate range of pressure (0.7 Pa), where adatoms obtain more energy by ion bombardment, the adatoms can move more actively, and the portion of (4 0 0)-oriented grains will be increased. With that condition, the texture development of thermodynamically favorable (4 0 0) planes may progress more actively since the development speed would be proportional to the number of adatoms that move to (4 0 0) grains from the surface of (2 2 2) or (2 1 1)-oriented grains.

The change in the relative portion of (2 2 2) grains with increasing sputtering power showed a similar U-shaped curve as shown in Fig. 7b. At low sputtering power density, the energy of Ar^+ ions which collide with the target surface is low due to a low discharge voltage. As a result, the average energy of sputtered atoms is expected to be low. Also, the supplied energy by ion bombardment will be low due to low ion density. Consequently, adatom mobility is quite low at very low sputtering power density. With increasing sputtering power density, the portion of (2 2 2) grains decreased until 2.25 W/cm^2, and increased again. This slight decrease of (4 0 0) orientation at high power density may be due to increased deposition rate. The diffusion length of adatoms is diminished at high power density since the adatoms are more likely to be buried by incident sputtered atoms before the adatoms find thermodynamically favorable sites. In fact, (2 2 2) orientation is very dominant for ITO films prepared by ion plating or pulsed laser deposition (PLD) technique, whose deposition rate is very high [8].

Substrate temperature can be a direct measure for adatom mobility. At high temperature, the adatoms have sufficient activation energy for generating the nuclei of (4 0 0) orientation. Fig. 8 clearly shows the relative peak intensity of the (4 0 0) plane increased as the deposition temperature increased.

On the other hand, Yu et al. proposed a model for the texture development of thin films based on the difference of sputtering yield with crystallographic orientation of grains [29]. They explained that grains with the lowest sputtering yield have the highest chance of surviving under re-sputtering conditions. In this study, however, ion energy could not be considerably changed by raising substrate temperatures or oxygen flow rates. As a result, the change of texture would not be able to be explained only from the difference of re-sputtering yield.

4. Conclusions

From the change of $\theta - 2\theta$ XRD profiles, ITO films deposited with no additional oxygen gas flow evolved to (4 0 0) orientation with increasing films thickness, which may be due to a lower surface energy and a height advantage combined with shadowing effect. On the other hand, 6 sccm of additional oxygen flow resulted in no (4 0 0) peak in XRD profiles, which denotes deposition conditions are very important for determining the crystallographic orientation of nuclei at the initial growth stage.

Sputtering variables such as oxygen flow rate, sputtering pressure, substrate temperature and sputtering power density significantly influenced the texture of ITO thin films. Less amounts of additional oxygen gas, moderate ranges of pressure and power density and higher substrate temperatures, where adatoms are expected to have higher mobility, resulted in more (4 0 0)-oriented film texture.

References

[1] G. Haacke, Annu. Rev. Mater. Sci. 7 (1977) 73.
[2] C.G. Granqvist, Appl. Phys. A 52 (83) (1991) 83.
[3] H. Sato, T. Minami, S. Takata, T. Miyata, M. Ishii, Thin Solid Films 102 (1983) 1.
[4] I. Hamberg, C.G. Grangvist, J. Appl. Phys. 60 (1986) R123.
[5] S. Ishibashi, Y. Higuchi, Y. Ota, K. Nakamura, J. Vac. Sci. Technol. A 8 (1990) 1403.
[6] P.K. Song, Y. Shigesato, I. Yasui, C.W. Ow-Yang, D. Paine, Jpn. J. Appl. Phys. 37 (1998) 1870.
[7] P.K. Song, Y. Shigesato, M. Kamei, I. Yasui, Jpn. J. Appl. Phys. 38 (1999) 2921.
[8] H. Kim, J.S. Horwitz, G. Kushto, A. Pique, Z.H. Kafafi, C.M. Gilmore, D.B. Chrisey, J. Appl. Phys. 88 (2000) 6021.
[9] H. Izumi, F.O. Adurodija, T. Kaneyoshi, T. Ishihara, H. Yoshioka, M. Motoyama, J. Appl. Phys. 91 (2002) 1213.
[10] F.E. Akkad, M. Marafi, A. Punnoose, G. Prabu, Phys. Stat. Sol. 177 (2000) 445.
[11] P. Thilakan, J. Kumar, Vacuum 48 (1997) 463.
[12] Y.S. Jung, D.W. Lee, 2002, unpublished.
[13] R.W. Smith, J. Appl. Phys. 81 (1997) 1196.
[14] A. van der Drift, Philips Res. Rep. 22 (1967) 267.
[15] T.Q. Li, S. Noda, T.T. Ohsawa, H. Komiyama, J. Vac. Sci. Technol. A 20 (2002) 583.
[16] J. Pelleg, L.Z. Zevin, S. Lungo, Thin Solid Films 197 (1991) 117.
[17] R. Banerjee, R. Chandra, P. Ayyub, Thin Solid Films 405 (2002) 64.
[18] J.E. Green, J.-F. Sundgren, L. Hultman, I. Petrov, D.B. Bergstrom, Appl. Phys. Lett. 67 (1995) 2928.
[19] F. Ying, R.W. Smith, D.J. Srolovitz, Appl. Phys. Lett. 69 (1996) 3007.
[20] C.G. Choi, K. No, W.J. Lee, H.G. Kim, S.O. Jung, W.J. Lee, W.S. Kim, S.J. Kim, C. Yoon, Thin Solid Films 258 (1995) 274.
[21] J.A. Thornton, Rev. Mater. Sci. 7 (1977) 239.
[22] A.V.D. Drift, Philips. Res. Repts. 22 (1967) 267.
[23] M. Ohring, The Material Science of Thin Films. Academic Press, San Diego, 1992, p. 227.
[24] M. Kamei, Y. Shigesato, S. Takaki, Thin Solid Films 259 (1995) 38.
[25] C.H. Yi, I. Yasui, Y. Shigesato, Jpn. J. Appl. Phys. 34 (1995) 1638.
[26] M. Ohring, The Material Science of Thin Films. Academic Press, San Diego, 1992, p. 202.
[27] K.-F. Chiu, Z.H. Barber, Thin Solid Films 358 (2000) 264.
[28] S. Mader, R. Giang, L.T. Maissel, Handbook of Thin Film Technology. McGraw-Hill, New York, 1970, p. 21.
[29] L.S. Yu, J.M.E. Harper, J.J. Cuomo, D.A. Smith, Appl. Phys. Lett. 47 (1985) 932.